

Supporting Information for

**Gold(I) *N*-heterocyclic carbene complexes with tunable electronic properties for sensitive colorimetric detection of glutathione**

Yi-Fan Zhang,<sup>a,b</sup> Xin Li,<sup>b</sup> Heng Zhang,<sup>b</sup> Xi-Qiang Wang,<sup>a</sup> Li-Ying Sun,<sup>b</sup> Xiang-Long Duan<sup>\*ac</sup> and Ying-Feng Han<sup>\*b</sup>

<sup>a</sup> Second Department of General Surgery, Shaanxi Provincial People's Hospital, Xi'an, 710068 Shaanxi, China.

<sup>b</sup> Key Laboratory of Synthetic and Natural Functional Molecule of the Ministry of Education, Xi'an Key Laboratory of Functional Supramolecular Structure and Materials, College of Chemistry and Materials Science, Northwest University, Xi'an, 710127 Shaanxi, China.

<sup>c</sup> Institute of Medical Research, Northwestern Polytechnical University Xi'an 710072 Shaanxi, China, Third Affiliated Hospital of Xi'an Jiaotong University, Xi'an, 710068 Shaanxi, China.

E-mail: yfhan@nwu.edu.cn, duanxianglong@nwpu.edu.cn

**Table of Contents:**

1. NMR spectrum of complex <b>1–4</b>	S1
2. X-ray crystallography for <b>1–4</b>	S7
3. Time-dependent absorbance changes at 652 nm of TMB	S12
4. The catalytic activity of complexes depends on pH and temperature	S13
5. The stability studies of complexes under different pH	S14
6. EPR spectra of different reaction samples	S14
7. Intracellular ROS detection and Cytotoxicity	S16
8. Cyclic voltammograms of complexes <b>1–4</b>	S18
9. Colorimetric detection of H <sub>2</sub> O <sub>2</sub>	S18
10. Comparison of Au(I)-NHC complex <b>1</b> and other colorimetric methods for GSH detection	S18
11. Cartesian coordinates of the optimized geometries	S19
12. References	S24

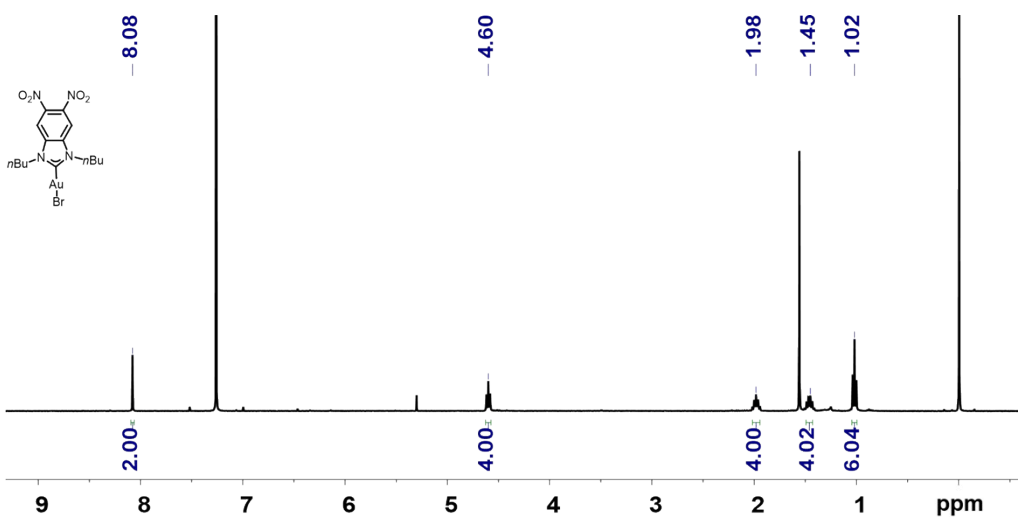


**Fig. S1.** <sup>1</sup>H NMR spectrum of complex **1** (400 MHz, CDCl<sub>3</sub>).

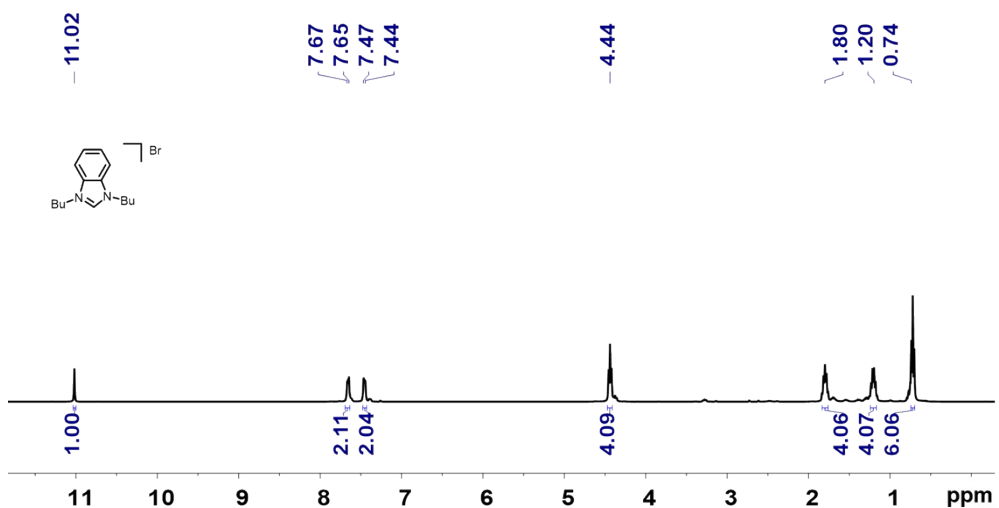


**Fig. S2.** <sup>1</sup>H NMR spectrum of 1,3-dibutylbenzoimidazolium bromide (400 MHz, DMSO-d<sub>6</sub>).

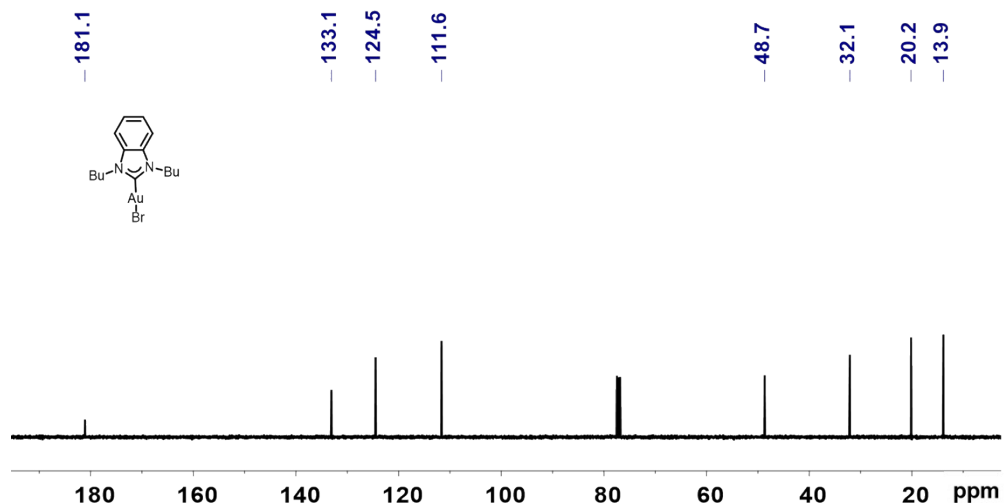
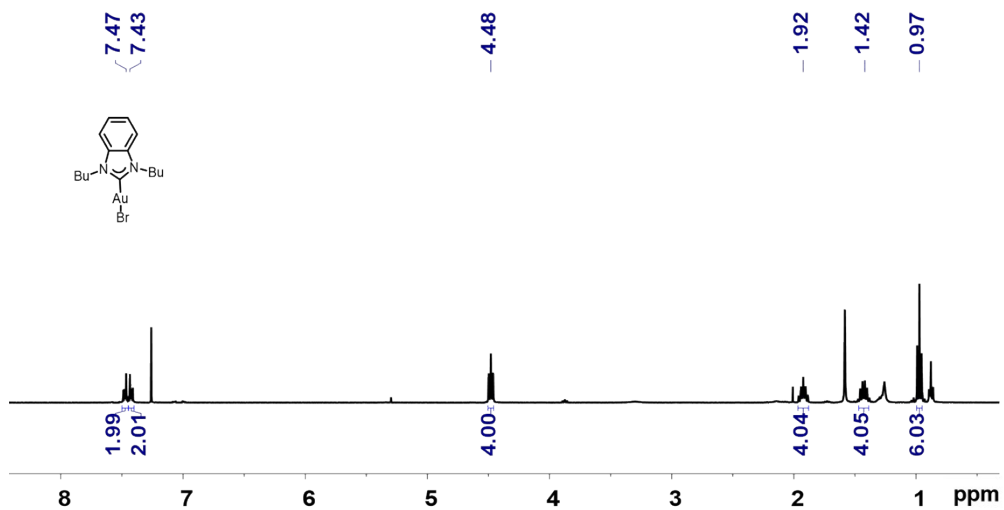


**Fig. S4.**  $^{13}\text{C}$  NMR spectrum of complex **2** (150 MHz,  $\text{CDCl}_3$ ).

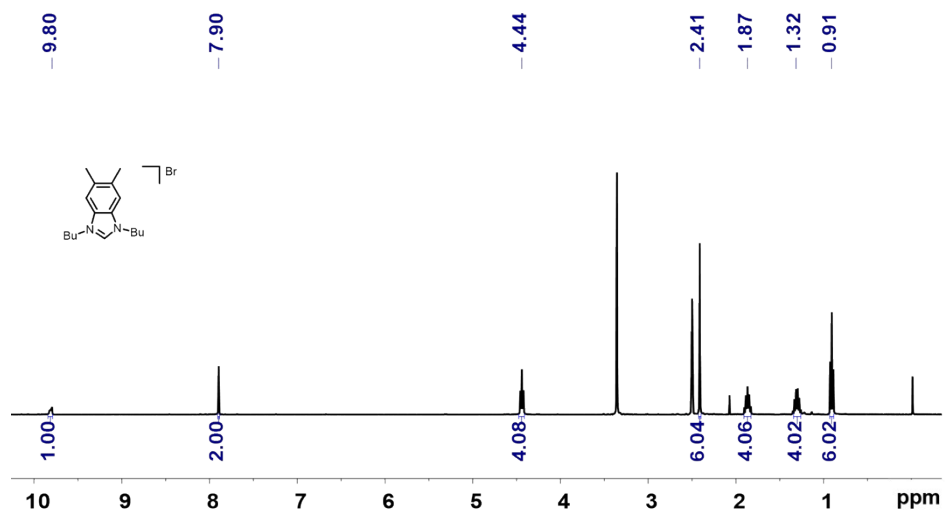


**Fig. S5.**  $^1\text{H}$  NMR spectrum of 1,3-dibutyl-5,6-dimethyl-benzoimidazolium bromide (400 MHz,  $\text{DMSO}-d_6$ ).

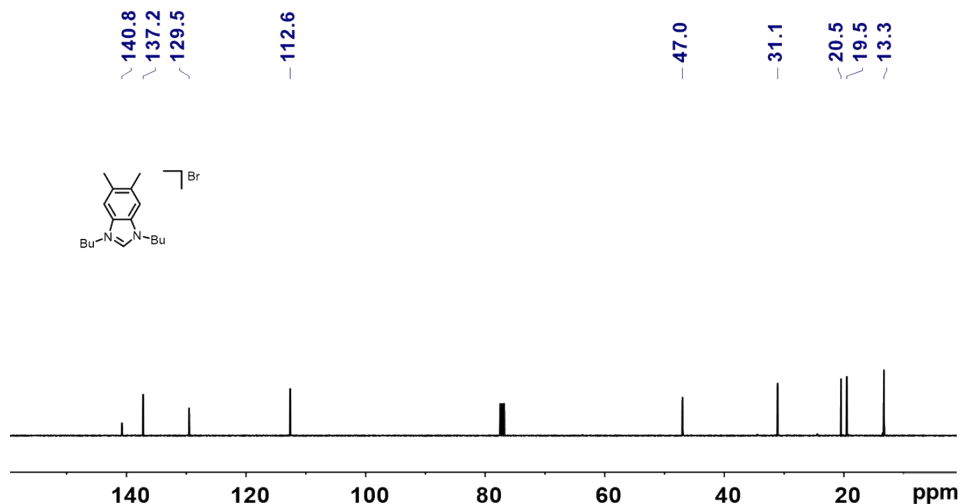


**Fig. S6.**  $^{13}\text{C}$  NMR spectrum of 1,3-dibutyl-5,6-dimethyl-benzoimidazolium bromide (150 MHz,  $\text{DMSO}-d_6$ ).

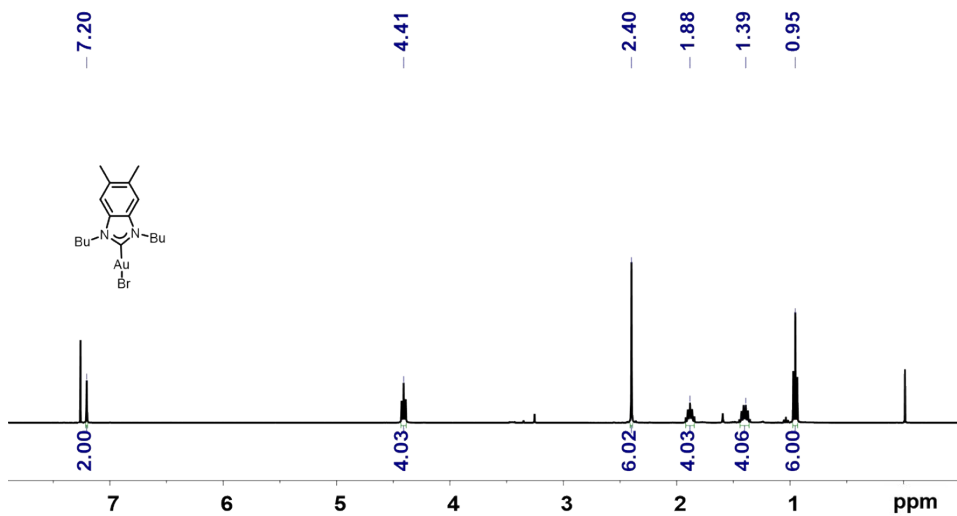


**Fig. S7.** <sup>1</sup>H NMR spectrum of complex **3** (400 MHz, CDCl<sub>3</sub>).

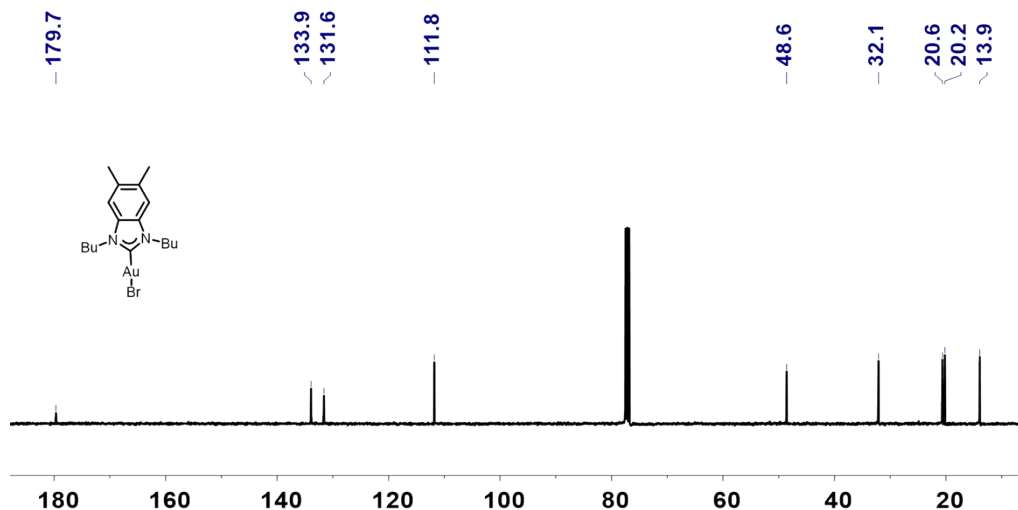


**Fig. S8.** <sup>13</sup>C NMR spectrum of complex **3** (150 MHz, CDCl<sub>3</sub>).

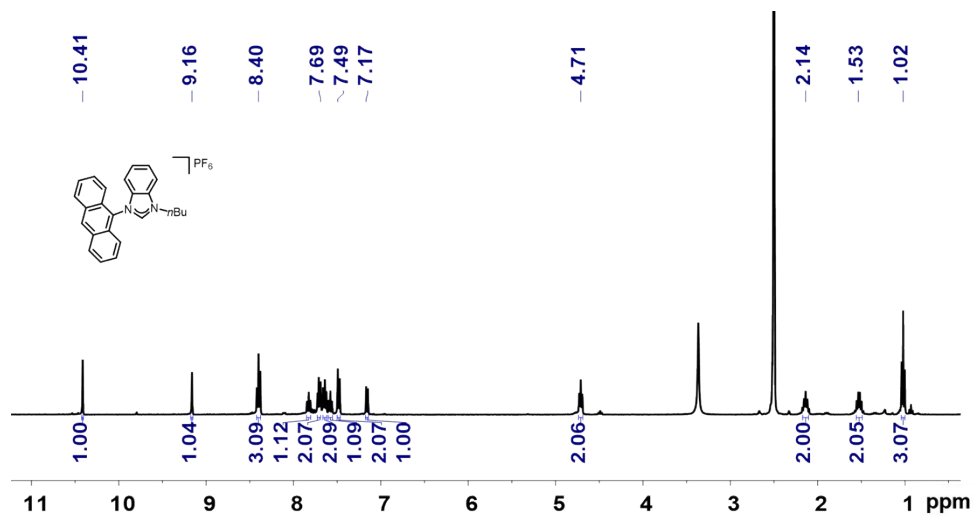


**Fig. S9.**  $^1\text{H}$  NMR spectrum of *N*-(9-anthracyl)-*N'*-(butyl)-benzimidazolium bromide (400 MHz,  $\text{DMSO}-d_6$ ).

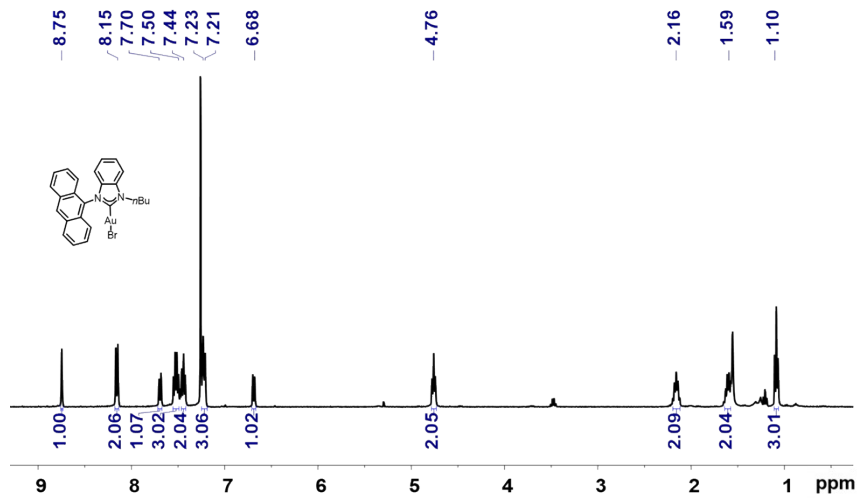


**Fig. S10.**  $^1\text{H}$  NMR spectrum of complex **4** (400 MHz,  $\text{CDCl}_3$ ).

**Table S1.** Crystallographic data and the structure refinement details for **1**.

Empirical formula	C <sub>15</sub> H <sub>20</sub> AuBrN <sub>4</sub> O <sub>4</sub>
Formula weight	597.23
Temperature/K	228.0
Crystal system	monoclinic
Space group	P2 <sub>1</sub> /n
a/Å	14.3250(7)
b/Å	8.8390(4)
c/Å	14.6957(8)
α/°	90
β/°	93.103(2)
γ/°	90
Volume/Å <sup>3</sup>	1858.02(16)
Z	4
ρ <sub>calc</sub> (g/cm <sup>3</sup> )	2.135
μ (mm <sup>-1</sup> )	10.095
F (000)	1136.0
Crystal size/mm <sup>3</sup>	0.3 × 0.28 × 0.27
Radiation	Mo Kα ( $\lambda = 0.71073$ )
2θ range for data collection/°	5.38 to 52.784
Index ranges	-17 ≤ h ≤ 16, -11 ≤ k ≤ 11, -18 ≤ l ≤ 18
Reflections collected	12793
Independent reflections	3804 [ $R_{\text{int}} = 0.0293$ , $R_{\text{sigma}} = 0.0323$ ]
Data/restraints/parameters	3804/0/228
Goodness-of-fit on $F^2$	1.132
Final R indexes [I ≥ 2σ (I)]	$R_1 = 0.0273$ , $wR_2 = 0.0573$
Final R indexes [all data]	$R_1 = 0.0334$ , $wR_2 = 0.0591$
Largest diff. peak/hole / e Å <sup>-3</sup>	0.90/-0.64
CCDC	2239763

**Table S2.** Crystallographic data and the structure refinement details for **2**.

Empirical formula	C <sub>15</sub> H <sub>22</sub> AuBrN <sub>2</sub>
Formula weight	507.22
Temperature/K	200.00
Crystal system	orthorhombic
Space group	<i>Pbcn</i>
<i>a</i> /Å	21.5840(7)
<i>b</i> /Å	8.8563(2)
<i>c</i> /Å	17.1841(6)
$\alpha/^\circ$	90
$\beta/^\circ$	90
$\gamma/^\circ$	90
Volume/Å <sup>3</sup>	3284.82(17)
<i>Z</i>	8
$\rho_{\text{calc}}$ (g/cm <sup>3</sup> )	2.051
$\mu$ (mm <sup>-1</sup> )	11.380
<i>F</i> (000)	1920.0
Crystal size/mm <sup>3</sup>	0.32 × 0.3 × 0.29
Radiation	Mo <i>K</i> α ( $\lambda = 0.71073$ )
2 <i>θ</i> range for data collection/°	5.102 to 52.826
Index ranges	-26 ≤ <i>h</i> ≤ 22, -11 ≤ <i>k</i> ≤ 9, -13 ≤ <i>l</i> ≤ 21
Reflections collected	10435
Independent reflections	3343 [ $R_{\text{int}} = 0.0219$ , $R_{\text{sigma}} = 0.0237$ ]
Data/restraints/parameters	3343/0/174
Goodness-of-fit on <i>F</i> <sup>2</sup>	1.035
Final R indexes [ <i>I</i> ≥ 2σ ( <i>I</i> )]	$R_1 = 0.0180$ , $wR_2 = 0.0380$
Final R indexes [all data]	$R_1 = 0.0229$ , $wR_2 = 0.0393$
Largest diff. peak/hole / e Å <sup>-3</sup>	0.35/-0.67

**Table S3.** Crystallographic data and the structure refinement details for **3**.

Empirical formula	C <sub>17</sub> H <sub>26</sub> AuBrN <sub>2</sub>
Formula weight	535.27
Temperature/K	222.00
Crystal system	tetragonal
Space group	P4 <sub>2</sub> /n
a/Å	12.1551(9)
b/Å	12.1551(9)
c/Å	28.806(3)
α/°	90
β/°	90
γ/°	90
Volume/Å <sup>3</sup>	4255.9(7)
Z	8
ρ <sub>calc</sub> (g/cm <sup>3</sup> )	1.671
μ (mm <sup>-1</sup> )	8.788
F (000)	2048.0
Crystal size/mm <sup>3</sup>	0.23 × 0.21 × 0.18
Radiation	Mo Kα ( $\lambda = 0.71073$ )
2θ range for data collection/°	3.636 to 52.094
Index ranges	-14 ≤ h ≤ 14, -15 ≤ k ≤ 12, -35 ≤ l ≤ 35
Reflections collected	41503
Independent reflections	4138 [ $R_{\text{int}} = 0.0889$ , $R_{\text{sigma}} = 0.0508$ ]
Data/restraints/parameters	4138/269/203
Goodness-of-fit on $F^2$	1.100
Final R indexes [I ≥ 2σ (I)]	$R_1 = 0.1478$ , $wR_2 = 0.3342$
Final R indexes [all data]	$R_1 = 0.1805$ , $wR_2 = 0.3510$
Largest diff. peak/hole / e Å <sup>-3</sup>	3.14/-2.13
CCDC	2239764

**Table S4.** Crystallographic data and the structure refinement details for **4**.

Empirical formula	C <sub>26</sub> H <sub>24</sub> AuBrCl <sub>2</sub> N <sub>2</sub>
Formula weight	712.25
Temperature/K	200.00
Crystal system	triclinic
Space group	P <sup>1</sup>
<i>a</i> /Å	10.3079(5)
<i>b</i> /Å	11.3455(6)
<i>c</i> /Å	12.2406(7)
$\alpha/^\circ$	111.256(2)
$\beta/^\circ$	104.585(2)
$\gamma/^\circ$	90.394(2)
Volume/Å <sup>3</sup>	1283.47(12)
<i>Z</i>	2
$\rho_{\text{calc}}$ (g/cm <sup>3</sup> )	1.843
$\mu$ (mm <sup>-1</sup> )	7.512
<i>F</i> (000)	684.0
Crystal size/mm <sup>3</sup>	0.3 × 0.28 × 0.26
Radiation	Mo <i>K</i> α ( $\lambda = 0.71073$ )
2 <i>θ</i> range for data collection/°	4.726 to 51.272
Index ranges	-11 ≤ <i>h</i> ≤ 12, -13 ≤ <i>k</i> ≤ 13, -14 ≤ <i>l</i> ≤ 14
Reflections collected	19305
Independent reflections	4821 [ $R_{\text{int}} = 0.0412$ , $R_{\text{sigma}} = 0.0400$ ]
Data/restraints/parameters	4821/13/290
Goodness-of-fit on <i>F</i> <sup>2</sup>	1.032
Final R indexes [ <i>I</i> ≥ 2σ ( <i>I</i> )]	$R_1 = 0.0309$ , $wR_2 = 0.0689$
Final R indexes [all data]	$R_1 = 0.0378$ , $wR_2 = 0.0723$
Largest diff. peak/hole / e Å <sup>-3</sup>	1.18/-1.19
CCDC	2239765

**Table S5.** Important bond distances and angles of Au(I)-NHC complexes **1–4**.

Complex		<b>1</b>	<b>2</b>	<b>3</b>	<b>4</b>
distance (Å)	C <sub>NHC</sub> -Au(1)	1.980(5)	1.988(3)	1.962(13)	1.983(5)
	Au(1)-Br(1)	2.476(6)	2.397(3)	2.357(5)	2.392(6)
Angle ° C <sub>NHC</sub> -Au-Br		178.14(13)	179.27(9)	179.10(6)	178.25(14)

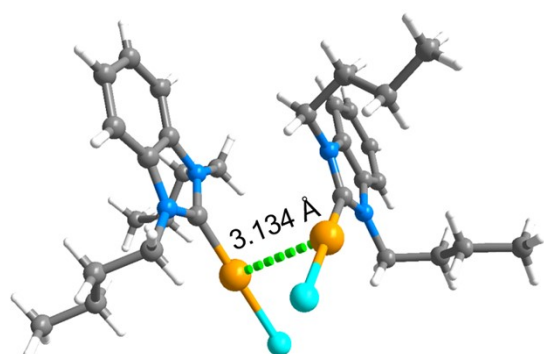


**Fig. S11.** The Au–Au interactions (3.134 Å) observed between the neighbouring complex **2**.

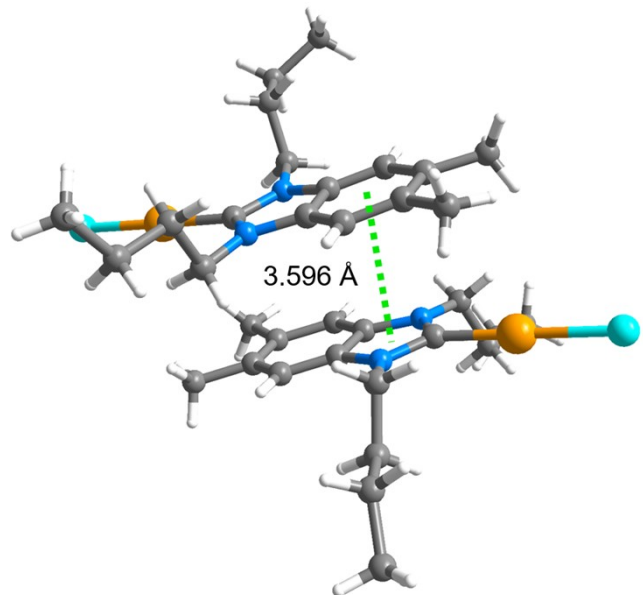


**Fig. S12.** The  $\pi$ – $\pi$  stacking interactions (3.596 Å) observed between phenyl rings and imidazoline-2-ylidene of neighboring structure of complex **3**.

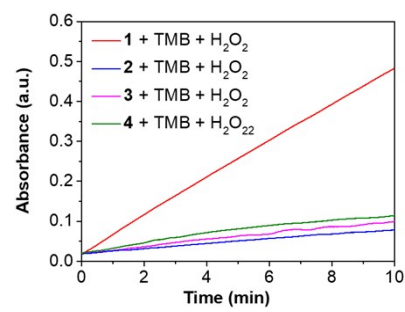


**Fig. S13.** Time-dependent absorbance changes at 652 nm of TMB catalysed by complexes **1–4**.

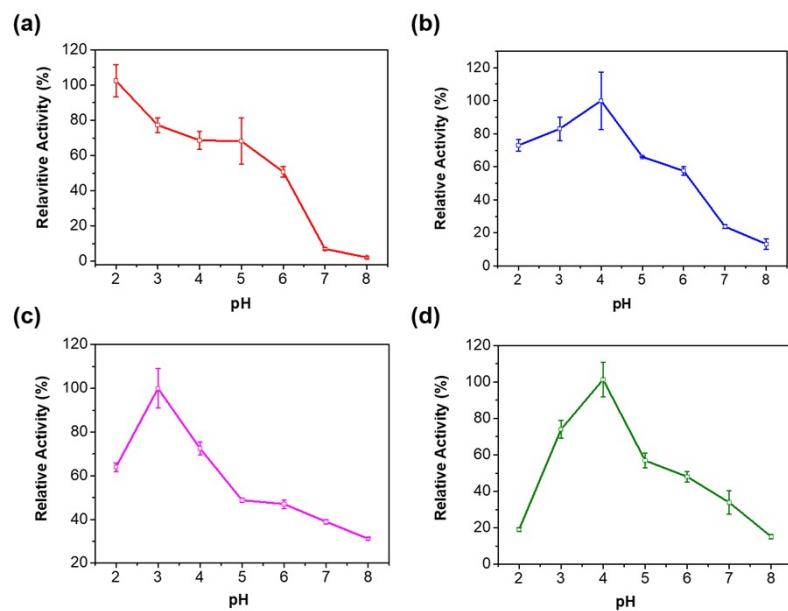


**Fig. S14.** The catalytic activity of Au-NHC complexes depends on pH, complex **1** (a), **2** (b), **3** (c), and **4** (d).

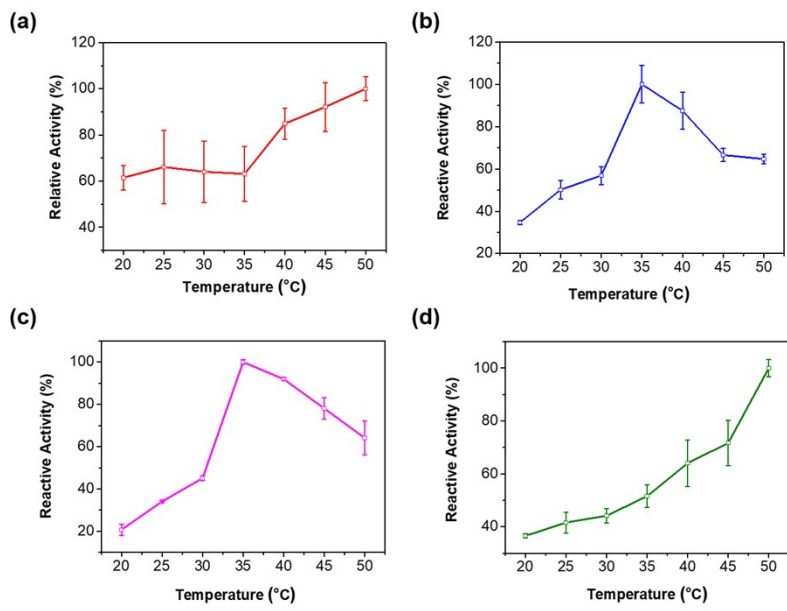


**Fig. S15.** The catalytic activity of Au-NHC complexes depends on temperature, complex **1** (a), **2** (b), **3** (c), and **4** (d).

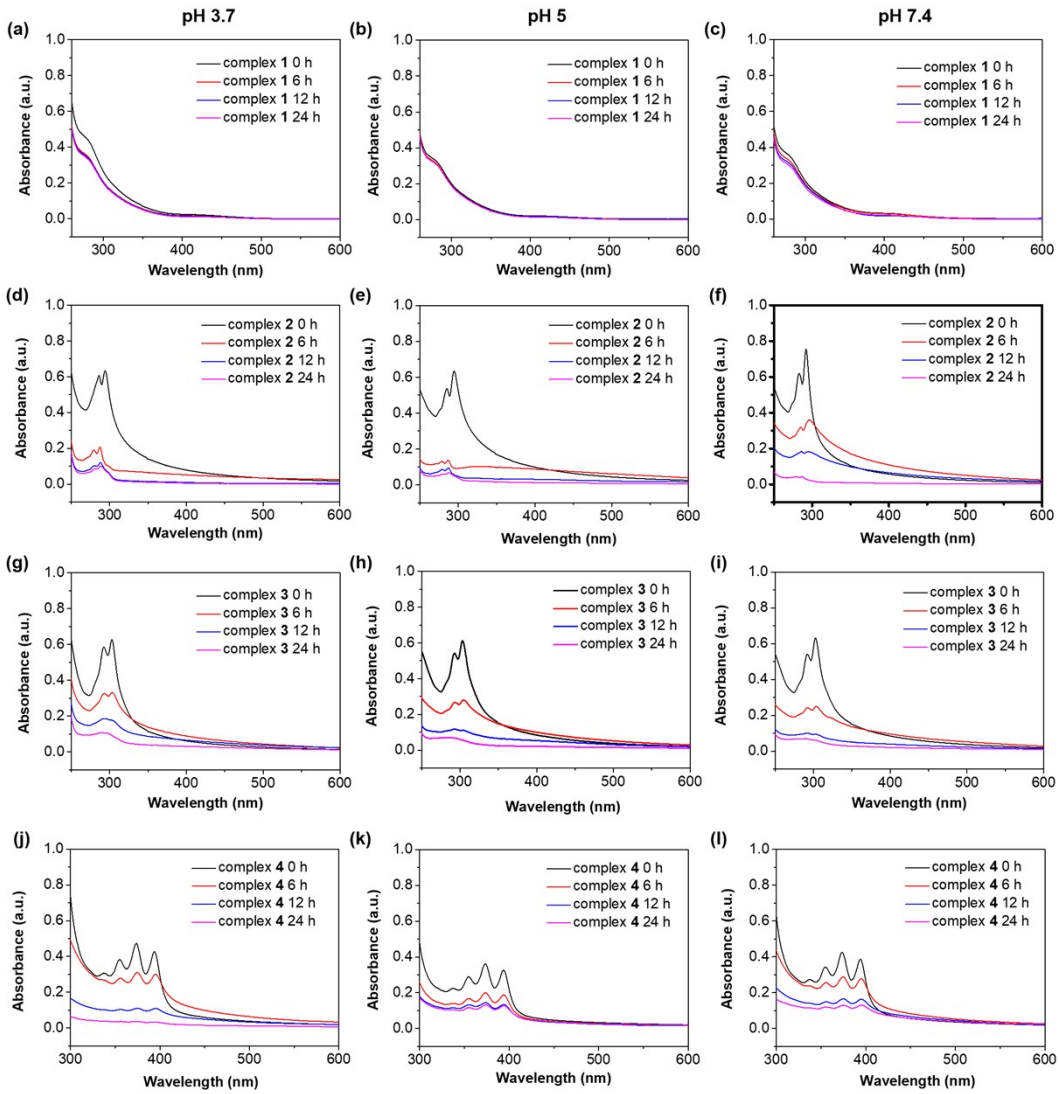


**Fig. S16.** UV-vis spectra of complexes **1–4** under different pH buffers.

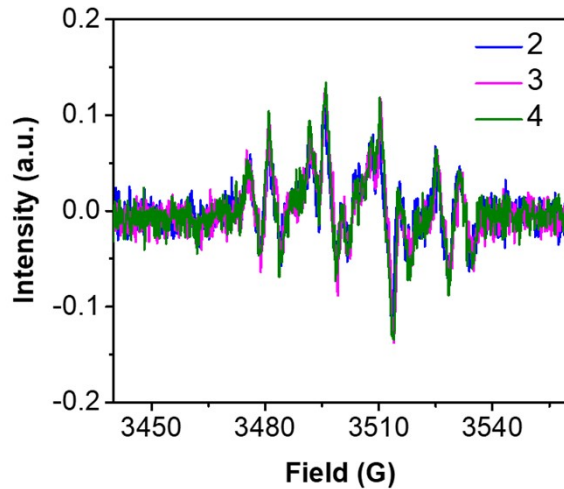


**Fig. S17.** EPR spectra of different reaction samples with DMPO (100 mM) as the spin trap.  $[H_2O_2] = 0.5\text{ M}$ .

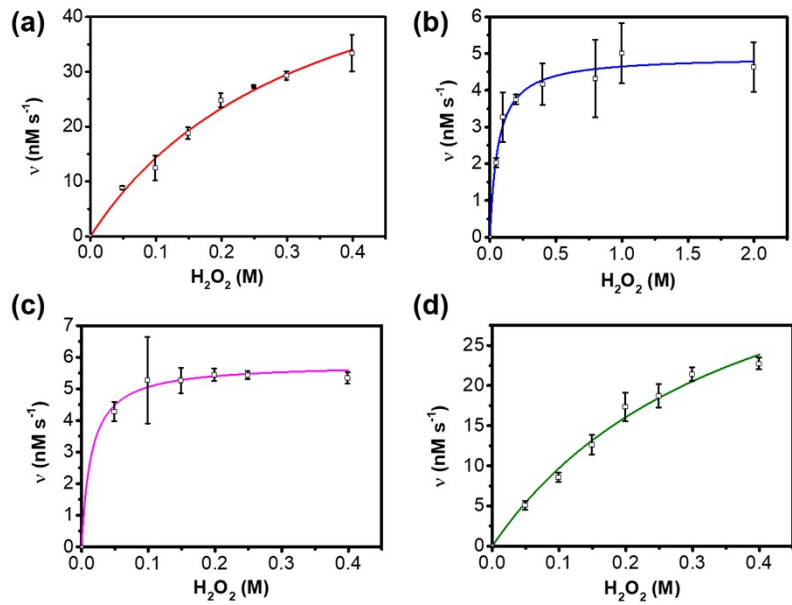


**Fig. S18.** Michaelis-Menten curve of Au(I)-NHC complexes 1–4 under different concentrations of  $\text{H}_2\text{O}_2$ , respectively. complex **1** (a), **2** (b), **3** (c), and **4** (d).

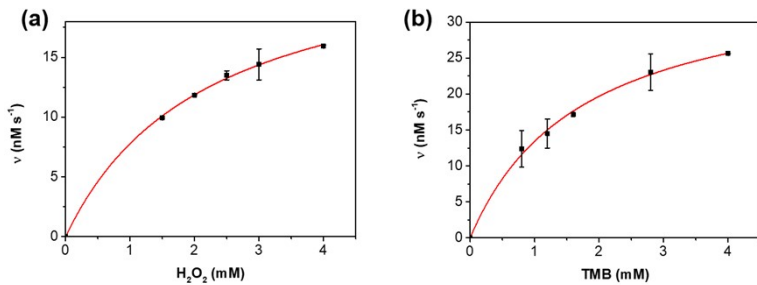


**Fig. S19.** Michaelis-Menten curve of HRP under different concentrations of  $\text{H}_2\text{O}_2$  and TMB, respectively.

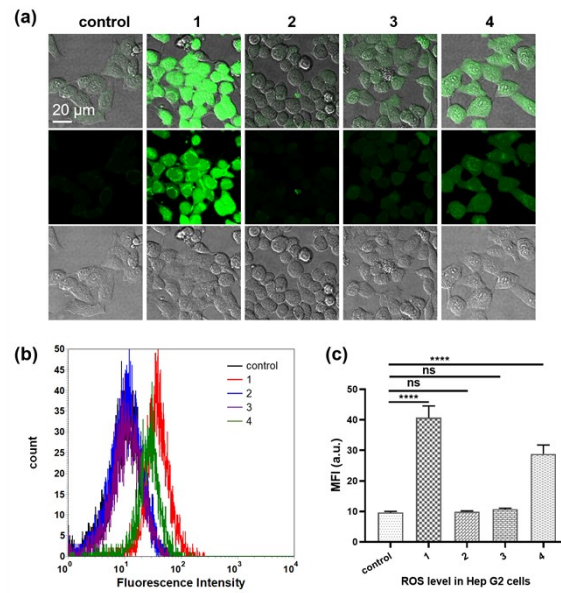


**Fig. S20.** Intracellular ROS detection of Hep G2 cells after Au(I)-NHC complexes treatment for 4 h by (a) CLSM images and (b) flow cytometry. (c) Quantization of ROS level of Hep G2 cells treated with Au(I)-NHC complexes.

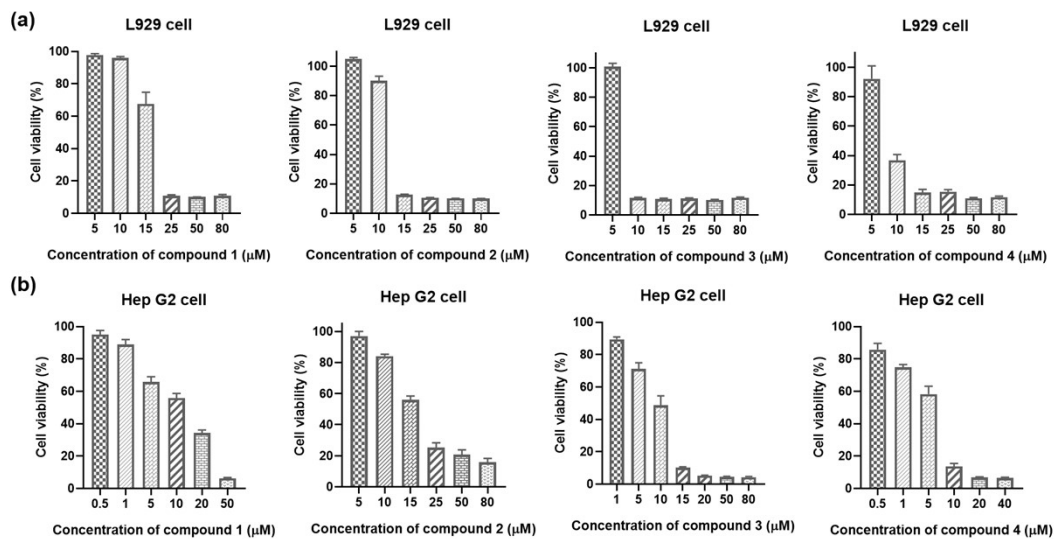


**Fig. S21.** Cytotoxicity of complexes 1–4 against L929 and Hep G2 cells.

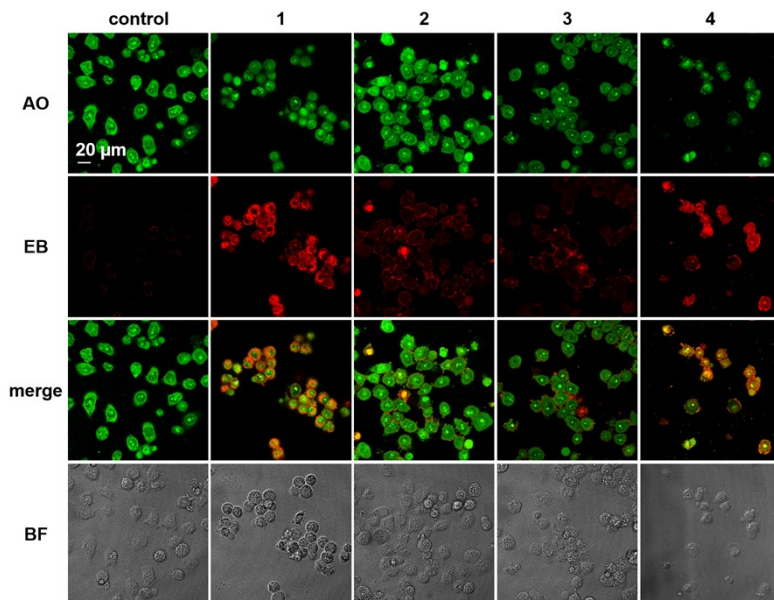


**Fig. S22.** Live/dead cell staining using acridine orange (AO, green emission for living cells) and ethidium bromide (EB, red emission for dead cells) assays after different treatments.

**Table S6** IC<sub>50</sub> values of **1–4** against Hep G2 and L929 cells after 24 h co-incubation.

IC <sub>50</sub> μM	<b>1</b>	<b>2</b>	<b>3</b>	<b>4</b>
Hep G2	9.95 ± 0.56	14.61 ± 0.32	10.39 ± 0.47	5.95 ± 0.25
L929	16.21 ± 0.42	11.34 ± 0.16	7.45 ± 0.94	8.93 ± 0.54
Selectivity index <sup>a</sup>	1.63	0.78	0.72	1.50

<sup>a</sup>Selectivity index was determined by dividing the IC<sub>50</sub> value against L929 normal cells by the IC<sub>50</sub> against cancer cells.

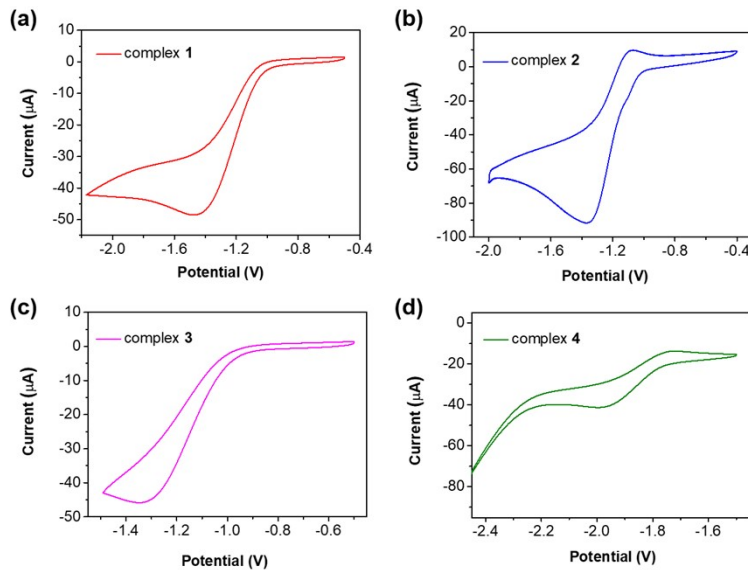


**Fig. S23.** Cyclic voltammograms of complexes **1–4**. ( $n\text{Bu}_4\text{NPF}_6$  in water,  $200 \text{ mV s}^{-1}$  vs  $\text{Ag}/\text{AgCl}$ ,  $c = 10^{-5} \text{ M}$ ).

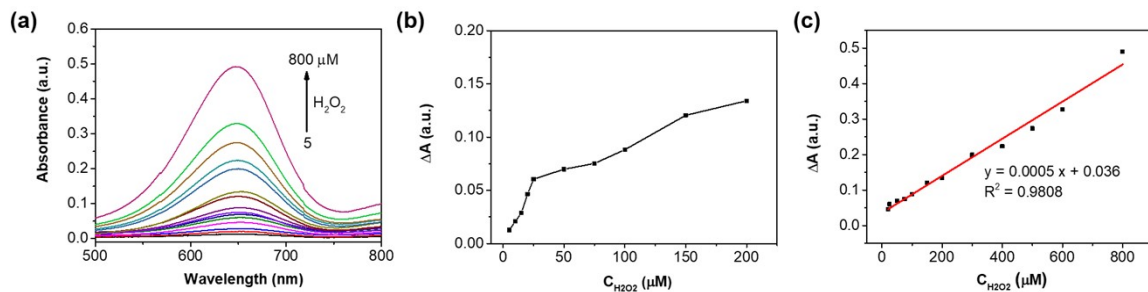


**Fig. S24.** (a) UV-vis absorption curves and (b) absorbance at 652 nm of [TMB + **1**] with various concentrations of  $\text{H}_2\text{O}_2$ . (c) linear calibration chart of  $\text{H}_2\text{O}_2$  detection.

**Table S7** Comparison of Au(I)-NHC complex **1** and other colorimetric methods for GSH detection.

Materials	Linear range ( $\mu\text{M}$ )	Detection limit( $\mu\text{M}$ )	Reference
MoS <sub>2</sub> nanoflakes	4.1–300	4.10	1
CuZnFeS nanocrystals	10–55	3	2
FeS <sub>2</sub> nanoparticles	2–80	0.91	3
Mn <sub>3</sub> O <sub>4</sub> microspheres	5–60	0.889	4
SPB-MnO <sub>2</sub>	0.5–12.5	0.45	5
Au nanoparticles	1–40	0.013	6
Py-TT COF	0.4–60	0.225	7
Co-POP	5–90	0.71	8
PSMOF	0–20	0.68	9

**Table S8** Cartesians coordinates of calculated (**1**) at the B3LYP/6-31G\*/LANL2DZ.

Atom	X	Y	Z
C	1.793522	0.658265	0.247776
C	1.79348	-0.65822	-0.24769
C	2.982873	-1.3338	-0.51303
C	4.16845	-0.65431	-0.26157
C	4.168477	0.654315	0.261519
C	2.982932	1.333834	0.513055
C	-0.35063	7.99E-05	0.000102
H	3.020058	-2.33928	-0.91344
H	3.020159	2.33931	0.913459
C	-0.00728	-2.34244	-0.83943
C	-0.11083	-3.35296	0.30823
H	0.683695	-2.68998	-1.6149
H	-0.98134	-2.18652	-1.30907
C	-0.60429	-4.72218	-0.17949
H	0.867944	-3.46086	0.795675
H	-0.80102	-2.95499	1.062949
C	-0.73407	-5.73955	0.958911
H	-1.57708	-4.59947	-0.6745
H	0.085326	-5.10972	-0.94275
H	-1.08879	-6.70529	0.583771
H	0.229611	-5.90702	1.454923
H	-1.44578	-5.3939	1.717661
C	-0.00724	2.342542	0.839568
C	-0.11106	3.352952	-0.30816
H	0.68386	2.690207	1.614879
H	-0.98119	2.186588	1.309401
C	-0.60433	4.72225	0.179547
H	0.867583	3.460747	-0.79589
H	-0.80149	2.954931	-1.06264
C	-0.73431	5.73953	-0.95891
H	-1.57701	4.599639	0.674798
H	0.085486	5.109811	0.942616

H	-1.08895	6.705308	-0.58377
H	0.229281	5.906955	-1.45511
H	-1.44616	5.39383	-1.7175
N	0.463472	1.02072	0.395366
N	0.463416	-1.02062	-0.3952
Au	-2.36881	2.81E-05	4.38E-05
N	5.408938	-1.32401	-0.69662
N	5.409015	1.323994	0.696505
O	6.263866	0.622281	1.222194
O	5.457147	2.542716	0.553759
O	5.457107	-2.54272	-0.55384
O	6.263749	-0.62231	-1.22243
Br	-4.81004	-0.00013	-0.00013

**Table S9** Cartesians coordinates of calculated (**2**) at the B3LYP/6-31G\*/LANL2DZ.

Atom	X	Y	Z
C	-2.85497756	0.64712895	-0.27321029
C	-2.85520961	-0.64651647	0.27333534
C	-4.04642943	-1.31828878	0.55353528
C	-5.23552745	-0.647643	0.27235783
C	-5.2352884	0.6490189	-0.27256692
C	-4.04593825	1.31928891	-0.55356767
C	-0.70428773	-0.00005269	0.00014257
H	-4.05198274	-2.32005591	0.97026347
H	-4.05109779	2.32106294	-0.97028559
C	-1.04760716	-2.30191271	0.92641567
C	-0.94935236	-3.35827661	-0.18003291
H	-1.7365382	-2.62013143	1.71657506
H	-0.07048149	-2.13510891	1.38641054
C	-0.46233163	-4.71093483	0.35669231
H	-1.92888791	-3.47775599	-0.66315018
H	-0.25790443	-2.99182329	-0.94942633
C	-0.33558109	-5.77104769	-0.74239673

H	0.51075276	-4.57500355	0.84792264
H	-1.15335435	-5.06761547	1.13405358
H	0.01378625	-6.72495726	-0.33260036
H	-1.29924732	-5.95115153	-1.2344722
H	0.37862427	-5.45652378	-1.51230571
C	-1.04678857	2.30190227	-0.92625018
C	-0.94863675	3.35851064	0.17997048
H	-1.73542693	2.62010275	-1.71667554
H	-0.06956684	2.13477705	-1.38591406
C	-0.46103976	4.71088692	-0.35696521
H	-1.92833629	3.47844191	0.66264221
H	-0.2576142	2.99217138	0.94982109
C	-0.33459833	5.77132858	0.74184393
H	0.51225174	4.57457541	-0.84767683
H	-1.1516151	5.06745682	-1.13477019
H	0.01530118	6.72499319	0.33193173
H	-1.2984907	5.95190867	1.23330425
H	0.3790624	5.45683478	1.51227157
N	-1.51599732	1.00210103	-0.43341769
N	-1.51635899	-1.00191591	0.43368488
Au	1.31877146	-0.00024172	0.00008326
H	-6.18220957	-1.13801096	0.47772324
H	-6.1817884	1.13967955	-0.47807203
Br	3.7705679	-0.00018344	-0.00005255

**Table S10** Cartesians coordinates of calculated (**3**) at the B3LYP/6-31G\*/LANL2DZ.

Atom	X	Y	Z
C	-2.43112606	0.64779324	-0.26491617
C	-2.43133006	-0.64709956	0.26482654
C	-3.62709191	-1.31338002	0.53399746
C	-4.83188567	-0.65892457	0.26844444
C	-4.83167934	0.66034524	-0.26860731
C	-3.62667919	1.31443803	-0.53412174

---

C	-0.28020537	0.00005932	0.00009798
H	-3.63175328	-2.32067883	0.93924994
H	-3.63101528	2.32173181	-0.93938887
C	-0.62522597	-2.31166039	0.90038125
C	-0.53247138	-3.35797271	-0.21619206
H	-1.31266607	-2.63663289	1.68922271
H	0.35374431	-2.15182936	1.35909479
C	-0.04731286	-4.71682105	0.30620724
H	-1.51374462	-3.47033457	-0.69749714
H	0.15759384	-2.98603311	-0.98420703
C	0.0743285	-5.76697154	-0.80299368
H	0.92732105	-4.58784591	0.79625155
H	-0.73714481	-5.07928597	1.08199442
H	0.42269151	-6.72555766	-0.40326351
H	-0.89098662	-5.94032414	-1.29437305
H	0.78716212	-5.44671617	-1.57184109
C	-0.62446501	2.3118854	-0.90022587
C	-0.53076441	3.35794311	0.21649463
H	-1.31211039	2.6373366	-1.6886844
H	0.35421168	2.15167266	-1.35943758
C	-0.04534988	4.71670535	-0.3059
H	-1.51177903	3.47059416	0.69825914
H	0.15952779	2.98565031	0.98414075
C	0.07710731	5.76662747	0.80342895
H	0.92904118	4.58746721	-0.79636191
H	-0.73537241	5.07953018	-1.08134801
H	0.42569537	6.72514289	0.40372696
H	-0.88795732	5.9402808	1.295194
H	0.79009789	5.44595304	1.57195386
N	-1.09225606	1.0069434	-0.42206233
N	-1.09257133	-1.00660768	0.42212728
Au	1.74330113	-0.0002278	0.00000772
C	-6.13780758	-1.36318873	0.5553555
H	-6.74540022	-0.81092565	1.28360622

---

H	-6.74963491	-1.47039378	-0.34950361
H	-5.9644126	-2.36480749	0.95962993
C	-6.13737964	1.36498694	-0.55559932
H	-6.74508441	0.81290008	-1.28389385
H	-6.74923347	1.47235671	0.34921868
H	-5.96367144	2.36655677	-0.9598583
Br	4.19668325	-0.00053585	-0.00020045

**Table S11** Cartesians coordinates of calculated (**4**) at the B3LYP/6-31G\*/LANL2DZ.

Atom	X	Y	Z
C	-0.4294543	2.69303509	-0.31260415
C	0.92588119	2.90659033	-0.60425838
C	1.42954046	4.19322394	-0.8057216
C	0.52620431	5.25048357	-0.70710662
C	-0.83306254	5.03188698	-0.41686422
C	-1.33591795	3.7477734	-0.21487236
C	0.60992164	0.67419768	-0.3687375
H	2.47725768	4.36838429	-1.02670802
H	-2.38232517	3.57037895	0.00882603
C	2.95237159	1.40050177	-0.86506476
C	3.78222937	1.48093165	0.42108371
H	3.29546256	2.13311516	-1.60389955
H	3.03768788	0.40835529	-1.31502784
C	5.27324561	1.22842504	0.16088434
H	3.64541498	2.46650832	0.88728279
H	3.39634117	0.7362856	1.1289582
C	6.11363408	1.28219665	1.44097818
H	5.39464158	0.2462151	-0.31557069
H	5.65087439	1.96950671	-0.55835846
H	7.17233725	1.10059506	1.22625598
H	6.03428718	2.26186511	1.92817777
H	5.78399274	0.52376306	2.16065775
N	-0.58352059	1.30937108	-0.17300801

N	1.52338727	1.64491032	-0.63743511
Au	0.94413738	-1.31109824	-0.25291848
H	0.88110451	6.26567755	-0.85688576
H	-1.50515996	5.88186963	-0.34828156
C	-1.82697124	0.65471475	0.13726669
C	-2.6580831	0.24343805	-0.92185808
C	-2.17301462	0.47163532	1.48949618
C	-3.91567933	-0.38873327	-0.59726016
C	-2.31843174	0.41638301	-2.29989254
C	-3.43545922	-0.1614807	1.79235017
C	-1.33679234	0.87673266	2.57626773
C	-4.76989755	-0.81233518	-1.66250221
C	-4.26706011	-0.57103522	0.74453256
C	-3.1680666	-0.00633936	-3.28899831
H	-1.37120583	0.87734933	-2.55726796
C	-3.80020815	-0.35376017	3.16123442
C	-1.72647878	0.67153357	3.87431973
H	-0.37996415	1.34054585	2.36320306
C	-4.41019813	-0.62723751	-2.97051977
H	-5.71250047	-1.29027196	-1.40808862
H	-5.21521405	-1.04924702	0.98044885
H	-2.89038023	0.12728486	-4.33071618
H	-4.75073613	-0.83434843	3.37845549
C	-2.97313771	0.05076321	4.17462063
H	-1.07519854	0.98023999	4.68716962
H	-5.06545362	-0.95686845	-3.77158045
H	-3.25902777	-0.10392015	5.21098177
Br	1.37889014	-3.72136127	-0.10957179

## References

1. J. Yu, D. Ma, L. Mei, Q. Gao, W. Yin, X. Zhang, L. Yan, Z. Gu, X. Ma, Y. Zhao, Peroxidase-Like Activity of MoS<sub>2</sub> Nanoflakes with Different Modifications and Their Application for H<sub>2</sub>O<sub>2</sub> and Glucose Detection, *J. Mater. Chem. B*, 2018, **6**, 487–498.

2. A. Dalui, B. Pradhan, U. Thupakula, A. H. Khan, G. S. Kumar, T. Ghosh, B. Satpati, S. Acharya, Insight into the Mechanism Revealing the Peroxidase Mimetic Catalytic Activity of Quaternary CuZnFeS Nanocrystals: colorimetric biosensing of hydrogen peroxide and glucose, *Nanoscale*, 2015, **7**, 9062–9074.
3. C. Song, W. Ding, W. Zhao, H. Liu, J. Wang, Y. Yao, C. Yao, High Peroxidase-like Activity Realized by Facile Synthesis of FeS<sub>2</sub> Nanoparticles for Sensitive Colorimetric Detection of H<sub>2</sub>O<sub>2</sub> and Glutathione, *Biosens. Bioelectron.*, 2020, **151**, 111983–8.
4. J. Xi, C. Zhu, Y. Wang, Q. Zhang, L. Fan, Mn<sub>3</sub>O<sub>4</sub> microspheres as an oxidase mimic for rapid detection of glutathione, *RSC Adv.*, 2019, **9**, 16509–16514.
5. Q. Yang, L. Li, F. Zhao, Y. Wang, Z. Ye, X. Guo, Generation of MnO<sub>2</sub> nanozyme in spherical polyelectrolyte brush for colorimetric detection of glutathione, *Mater. Lett.*, 2019, **248**, 89–92.
6. V. Kumar, D. Bano, D. K. Singh, S. Mohan, V. K. Singh, S. H. Hasan, Size-Dependent Synthesis of Gold Nanoparticles and Their Peroxidase-Like Activity for the Colorimetric Detection of Glutathione from Human Blood Serum, *ACS Sustainable Chem. Eng.*, 2018, **6**, 7662–7675.
7. G. Li, W. Ma, Y. Yang, C. Zhong, H. Huang, D. Ouyang, Y. He, W. Tian, J. Lin, Z. Lin, Nanoscale Covalent Organic Frameworks with Donor–Acceptor Structures as Highly Efficient Light-Responsive Oxidase-like Mimics for Colorimetric Detection of Glutathione, *ACS Appl. Mater. Interfaces*, 2021, **13**, 49482–49489.
8. D. Guo, C. Li, G. Liu, X. Luo, F. Wu, Oxidase Mimetic Activity of a Metalloporphyrin-Containing Porous Organic Polymer and Its Applications for Colorimetric Detection of Both Ascorbic Acid and Glutathione, *ACS Sustainable Chem. Eng.*, 2021, **9**, 5412–5421.
9. Y. Liu, M. Zhou, W. Cao, X. Wang, Q. Wang, S. Li, H. Wei, Light-Responsive Metal-Organic Framework as an Oxidase Mimic for Cellular Glutathione Detection, *Anal. Chem.*, 2019, **91**, 8170–8175.